
Article:
Oates, Caryn N., Denby, Katherine orcid.org/0000-0002-7857-6814, Myburg, Alexander A. et al. (2 more authors) (2020) Insect egg-induced physiological changes and transcriptional reprogramming leading to gall development. Plant, Cell and Environment. ISSN 0140-7791

https://doi.org/10.1111/pce.13930

Insect egg-induced physiological changes and transcriptional reprogramming leading to gall formation

Caryn N. Oates [1], Katherine J. Denby [2], Alexander A. Myburg [1], Bernard Slippers [1] and Sanushka Naidoo [1]

[1]Department of Biochemistry, Genetics and Microbiology, Forestry and Agricultural Biotechnology Institute (FABI), University of Pretoria, Private Bag x20, Pretoria 0028, South Africa

[2]Department of Biology, University of York, Wentworth Way, York YO10 5DD, UK;
katherine.denby@york.ac.uk

Corresponding author: Sanushka Naidoo
sanushka.naidoo@up.ac.za
+27 12 420 4974

Abstract

Gall-inducing insects and their hosts present some of the most intricate plant-herbivore interactions. Oviposition on the host is often the first cue of future herbivory and events at this early time point can affect later life stages. Many gallers are devastating plant pests, yet little information regarding the plant-insect molecular interplay exists, particularly following egg deposition. We studied the physiological and transcriptional responses of *Eucalyptus* following oviposition by the gall-inducing wasp, *Leptocybe invasa*, to explore potential mechanisms governing defence responses and gall development. RNA sequencing and microscopy were used to explore a susceptible *Eucalyptus-L. invasa* interaction. Infested and control material was compared over time (1-3, 7 and 90 days post oviposition) to examine the transcriptional and morphological changes. Oviposition induces accumulation of ROS and phenolics which is reflected in the transcriptome analysis. Gene expression supports phytohormones and ten transcription factor subfamilies as key regulators. The egg and oviposition fluid stimulate cell division resulting in gall development. *Eucalyptus* responses to oviposition are apparent within 24 hours. Putative defences include the oxidative burst and barrier reinforcement. However, egg and oviposition fluid stimuli may redirect these responses towards gall development.

Keywords: Developmental regulation, *Eucalyptus*, gall insect, *Leptocybe invasa*, oviposition, plant cell redifferentiation, plant defence, transcription factor

Introduction

Plants and insects have co-existed for hundreds of millions of years whichh has led to a wide variety of interactions between these organisms (Erb & Reymond, 2019). One of the most intricate relationships is the ability of some insect species to deposit their eggs and induce galls on their hosts. Galls are abnormal plant growths that are formed by active redifferentiation of plant tissues and provide the developing insect with superior nourishment and protection (Stone & Schönrogge, 2003). To defend themselves, plants have evolved a complex immune system comprising constitutive and inducible components. Constitutive defences are preformed physical or chemical barriers with insecticidal or antixenotic activity, whilst inducible defences are activated following recognition of elicitors (Jones & Dangl, 2006; Erb & Reymond, 2019).

In many cases, plant-galling insect interactions begin with oviposition on the host (Reymond, 2013). The site of egg deposition, including the accompanying oviposition fluid, on the leaf surface is an important interface where the first cues of imminent herbivory are perceived (Hilker & Fatouros, 2015). Different molecules may be recognised by the plant leading to the onset of induced immune responses, including herbivore-, egg- and damage-associated molecular patterns (HAMPs, EAMPs and DAMPs, respectively) as well as effectors (Boller & Felix, 2009; Hogenhout & Bos, 2011; Stuart, 2015). The latter are compounds secreted by the pest that mitigate the plant immune system and manipulate host physiology via specific host targets and are hypothesised to play key roles in plant-galling insect interactions (Deslandes & Rivas, 2012, Oates *et al.*, 2016). However, few causative molecules have been characterised in insect eggs or oviposition fluids, particularly for gall-inducing species.

Recognition is linked to the downstream defences by signalling machinery. Phytohormones, especially jasmonic acid (JA), salicylic acid (SA) and ethylene (ET), play central roles in organising defence against biotic stresses (Berens *et al.*, 2017). There is extensive crosstalk between hormone signalling pathways which provides a means of tailoring the immune system to the appropriate response (Erb *et al.*, 2012). JA is considered to be the primary regulator of plant resistance against insect herbivory (Erb & Reymond, 2019) as well as responses to egg deposition and associated wounding (Reymond, 2013). Up-regulation of JA biosynthesis- or signalling-related genes has been reported in response to oviposition by numerous insect species as well as EAMP treatment (Little *et al.*, 2006; Büchel *et al.*, 2012; Oates *et al.*, 2015) and is associated with increased egg mortality (Ament *et al.*, 2004).

Pest perception by a plant can cause extensive local cellular reprogramming aimed at neutralising the threat by direct and indirect defence mechanisms (Fürstenberg-Hägg *et al.*, 2013). Direct defences involve the synthesis of toxic compounds that act directly on the pest, whilst indirect defences involve the release of volatile signatures that attract the natural enemies of the pest (Unsicker *et al.*, 2009; Fürstenberg-Hägg *et al.*, 2013). A relatively small number of studies have examined plant responses to insect egg deposition, with fewer examining those induced by gallers. An array of defences has been reported in these studies including neoplasm development (Doss *et al.*, 2000) and production of larvicidal or ovicidal compounds (Fatouros *et al.*, 2015) as well as the release of volatile compounds that attract egg and/or larval parasitoids (Hilker *et al.*, 2002). Studies exploring plant resistance against galling insects have predominantly focused on larval life stages. To our knowledge, only one study has demonstrated induced terpene and transcriptome changes in response to the gall-inducing blue gum chalcid wasp (*Leptocybe invasa*) oviposition on *Eucalyptus* (Oates *et al.*, 2015).

The most commonly reported response to oviposition is the elicitation of a hypersensitive response (HR) (Hilker & Fatouros, 2016). The HR is preceded by a burst of reactive oxygen species (ROS) that induces the expression of pathogenesis-related (*PR*) genes and localised cell death at the site of egg deposition causing desiccation, detachment or is directly ovicidal (Balbyshev & Lorenzen, 1997; Geuss *et al.*, 2017; Griese *et al.*, 2017). ROS, along with effectors and phytohormones, have been proposed as important role players in gall initiation and development (Isaias *et al.*, 2015). The eggs and oviposition fluid of some galling species have been shown to stimulate redifferentiation and proliferation of adjacent host cells within days of deposition and occur alongside necrotic zones (Leggo & Shorthouse, 2006; Sliva & Shorthouse, 2006; Barnewall & de Clerck-Floate, 2012). This suggests that the pre-larval life stage is involved in the initiation of gall development. There is currently no comprehensive, molecular model that offers biological insight for any plant-galling insect species interaction. Future studies that clarify the mechanisms that govern resistance versus susceptibility will be imperative for the development of effective control measures against these pests.

Leptocybe invasa Fisher & La Salle (Hymenoptera: Eulophidae) is a gall-inducing pest of numerous, economically valuable *Eucalyptus* species and has achieved a global distribution since its discovery in 2000 (Mendel *et al.*, 2004; Dittrich-Schröder *et al*., 2018). It preferentially oviposits on immature shoot tips, midribs and petioles where successful larvae induce the formation of coalescing galls that may cause stunting, die-back or death (Mendel *et al.*, 2004). We previously examined the transcriptional reprogramming and induced changes in the terpene profile of resistant and susceptible *Eucalyptus* genotypes in response to *L. invasa* oviposition at seven days post infestation (dpi) (Oates *et al.*, 2015). This study showed that expression of genes associated with phytohormones, direct and indirect defences was altered in response to *L. invasa* oviposition. A study by Li *et al.*, (2017) explored concentration dynamics of selected compounds during *L. invasa*-induced gall development from oviposition to maturity. The study

105 examined the levels of carbon, nitrogen, phenolics, tannins and four phytohormones (auxins, cytokinins,
106 gibberellins (GA) and abscisic acid (ABA)) in two *Eucalyptus* genotypes varying in susceptibility to the gall
107 wasp. Interestingly, the results of the metabolite analysis at the pre-larval stage are reflected in the
108 transcriptomic responses described by Oates *et al.*, (2015).
109
110 Our previous study confirmed that the host *Eucalyptus* can identify the blue gum chalcid oviposition and
111 elicit defences that included alterations to the terpene profile. However, there is no information available
112 on the basic biology of the interaction such as where the egg and oviposition fluid are positioned or what
113 transcriptional and anatomical changes are induced that lead to gall formation. In this study, we
114 investigated *L. invasa* oviposition-induced physical and transcriptional responses of a susceptible
115 *Eucalyptus* hybrid clone over time.
116
117 **Materials and Methods**
118
119 *Infestation trial*
120
121 Two-year-old ramets of a susceptible (Dittrich-Schröder *et al.*, 2012) *Eucalyptus grandis* x *Eucalyptus*
122 *camaldulensis* hybrid clone (GC 540, Mondi) were coppiced and regrown in a *L. invasa*-proof field cage
123 insectarium. Ramets were divided into control and infested groups. For infested samples, newly emerged
124 *L. invasa* adults were collected in groups of five and exposed to selected target sites, which included the
125 shoot tip, the subsequent two immature leaves (≤ 3 cm in length) and the petiole at three target sites per
126 ramet (Figure 1). These sites were selected because they represent tissue that is preferentially targeted
127 by the gall wasp. A small plastic sleeve was tied around the target material to prevent wasp escape. The
128 wasps could oviposit from 11:00 to 12:00 before removal to ensure minimal diurnal variation was

introduced into the experiment. Control samples were not exposed to *L. invasa* but were otherwise treated equivalently. For transcriptome analysis, material was collected at 1, 2 and 3 dpi at 12:00 and immediately frozen in liquid nitrogen. Each time point included three biological replicates of control and infested samples. Each replicate was made up of material collected from three ramets. For microscopy analysis, material was collected at 1 hour post infestation (hpi) as well as 1, 2, 3, 7 and 90 dpi in triplicate as described for the transcriptomics.

Fixation and staining

For light microscopy, excised oviposition sites were fixed in formaldehyde, acetic acid and 50% ethanol (FAA, 1:1:18) (Berlyn *et al.*, 1976) and dehydrated in a butanolic series. Dehydrated samples were embedded in paraffin wax (Sigma-Aldrich), sectioned with a rotary microtome (10 µm) and attached to slides using Haupt's adhesive (1 g gelatine, 2 g phenol, 15 ml glycerine, 100 mL H_2O). Wax was removed using 100% xylene prior to staining. Sections were dual stained with Safranin O (uniLAB) and Fast Green FCF (uniLAB) before mounting in Entellan (Merck Millipore). The sections were photographed using a Carl Zeiss AG Axiocam ICc3 digital camera (Oberkochen, Germany) coupled to a light microscope (Carl Zeiss AG Axioskop) using Carl Zeiss AG AxioVision SE64 v4.9.0.0 software.

To measure H_2O_2 accumulation, whole infected and non-infected leaves were submerged in 3,3'-Diaminobenzidine tetrahydrochloride (DAB) Liquid Substrate solution (Sigma-Aldrich) for 4 hours. Leaves were destained by boiling in bleaching solution (ethanol, glacial acetic acid and glycerol, 3:1:1) at 95°C for 40 minutes and stored at 4°C. Leaves were photographed using an Olympus DP21 digital camera (Massachusetts, USA) coupled to a Nikon SMZ1500 dissecting microscope (Nikon Corp., Tokyo, Japan) using Olympus Stream Basic v1.9.4 software.

153

154 *RNA isolation and sequencing*

155

156 Infested and control samples were collected and immediately frozen in liquid nitrogen. Material was
157 excised approximately 5 mm around the oviposition sites whilst ensuring minimal thawing (Figure 1A).
158 The shoot tips, lower section of the midribs and petiole (the prospective oviposition sites) were excised
159 for control samples (Figure 1B, C). For 1 and 2 dpi control samples, these tissues were pooled (Figure 1B).
160 For the 3 dpi, these tissues were kept separately (Figure 1C). Total RNA was extracted using the Norgen
161 Plant/Fungi Total RNA Purification Kit (Norgen Biotek Corp.). Samples were treated using Qiagen RNase-
162 free DNase I enzyme (Qiagen Inc., Valencia, California, USA) and purified using the Qiagen RNeasy Mini
163 Kit and following the manufacturer's instructions. The concentration and quality of the RNA samples was
164 tested using the Bio-Rad Experion analyser (Bio-Rad, Hercules, USA). Total RNA was submitted to Beijing
165 Novogene Technology Co. Ltd. (Beijing, China) for mRNA-Seq analysis. The RNA libraries were prepared
166 using the TruSeq Stranded mRNA Library Prep Kit (Illumina Inc., San Diego, California, USA) with a 300 bp
167 insert. Samples were sequenced on the Illumina HiSeq 2500 platform in two batches with PE150 and
168 PE125 reads, respectively.

169

170 *Read mapping to the Eucalyptus v2.0 genome*

171

172 Read quality was analysed using FastQC v0.11.3 (Andrews 2010) and reads were trimmed using
173 Trimmomatic v0.32 (Bolger *et al.*, 2014) to ensure the mean and interquartile range per base sequence
174 quality scores were above a Phred score of 30 and the per base sequence content was passed. Reads were
175 aligned to the *E. grandis* v2.0 reference genome (Myburg *et al.*, 2014) using Tophat2 v2.0.14 (Kim *et al.*,
176 2013) and summarised using FeatureCounts v1.5.0-p3 (Liao *et al.*, 2014). DESeq2 v1.12.4 (Love *et al.*,

2014) was used to normalise the read counts using variance stabilising transformation and identify significantly differentially expressed genes (DEGs) in infested versus control samples (adjusted p-value ≤ 0.001) at each time point. DEGs at 3 dpi were calculated as infested versus all controls (ie. [INF] versus [ST, MR, PT]). DEGs were filtered for $\log_2$ fold changes ≥ 1.00 and ≤ -1.00 prior to further analysis. Data will be made available at https://eucgenie.org/.

Gene Ontology enrichment

Gene Ontology (GO) functional enrichment of up- and down-regulated DEGs was calculated with Fisher's exact test using all *E. grandis* v2.0 genes as a reference; p-values were corrected for multiple testing using the Benjamini and Hochberg false discovery rate (FDR) method (Benjamini & Hochberg, 1995). A corrected p-value of < 0.05 was used as a threshold to select enriched terms or pathways. The same approach was used to identify GO enrichment in network modules.

Transcription factor family analysis

Gene expression was analysed for 248 DEGs classified as TFs in the Plant Transcription Factor Database v4.0 (Jin *et al.*, 2014, 2015, 2017) and grouped by subfamily as defined by their associated *Arabidopsis thaliana* orthologues. Subfamilies overrepresented (adjusted p-value < 0.05) for DEGs at each time point, using all *E. grandis* v2.0 genes as a reference, were identified using the hypergeometric distribution with FDR correction (Benjamini & Hochberg, 1995).

Co-expression network modelling

Members of enriched TF subfamilies at the respective time point were selected as baits for gene co-expression network generation (Supplementary File S4.4). The analysis utilised an expression matrix incorporating data for all samples in this study as well as publicly available, pre-processed transcriptomic data from three prior studies of *Eucalyptus* biotic stress responses (https://eucgenie.org), including infection by *Phytophthora cinnamomi* (Meyer *et al.*, 2016), *Chrysoporthe austroafricana* (Mangwanda *et al.*, 2015) and infestation by *L. invasa* (Oates *et al.*, 2015). The co-expression network was generated using CoExpNetViz v1.0.2 (Tzfadia *et al.*, 2016) using the Pearson correlation coefficient method and filtered to include positive relationships between DEGs in the 95th percentile. Functional modules were identified using the MCL Cluster network partitioning algorithm from clusterMaker2 v1.2.1 (Morris *et al.*, 2011). Downstream modifications were completed using Cytoscape v3.6.1 (Shannon *et al.*, 2003).

Transcription factor binding site analysis

For transcription factor binding site (TFBS) analysis, 1500 bp upstream of the transcriptional start site of the network members was extracted. Sequences were filtered to ensure the promoter region did not overlap with preceding or succeeding genes and ≥100 bp in length. AME (Analysis of Motif Enrichment) v5.0.5 (http://meme-suite.org/) was used to identify known, enriched *Arabidopsis thaliana* motifs (E-value ≤ 0.0001, network cluster membership relative to whole genome) in the promoters as this is not currently available for *Eucalyptus*.

Results

Oviposition-induced cellular responses enable L. invasa *gall development*

225 Adult *L. invasa* females oviposit along the main vein on the ventral side of the plant tissue (Figure 2A, B
226 and Supplementary file S1). Scarring is apparent within one hour (1 hpi) of egg deposition and becomes
227 increasingly pronounced over time (Figure 2A and Supplementary file S1). ROS accumulation is co-
228 localised with the wound sites and increases in concentration from 1 to 3 dpi and appears stable until at
229 least 7 dpi (Figure 2A1-A5 and Supplementary file S1).
230
231 During each oviposition event, a channel is cut by the ovipositor and a single egg and oviposition fluid is
232 deposited into/near the plant vasculature (Figure 2B3-B5 and Supplementary file S1). The oviposition fluid
233 has a strong degradative effect on the surrounding tissue with cells showing thin/degraded cell walls
234 within an hour of exposure (Figure 2B3, B4) and is sustained over seven days. The newly laid egg is round
235 and possesses a long pedicel for anchorage (Figure 2B5). At 1-3 dpi, the developing embryo becomes
236 elongated and is roughly aligned with the vascular tissue vessels (Figure 2B6-B8). We also observed the
237 accumulation of phenolic compounds in the ventral cells at 1 dpi which was maintained over the entire
238 time series (Figure 2B6-B9, B11, B13). The phenolics appear to be co-localised with the ROS and the
239 oviposition-induced scarring (Figure 2A relative to Figure 2B and Supplementary file S1). At 7 dpi, there is
240 a clearly defined area of cell division parallel to the spread of the oviposition fluid in the host tissues
241 (Figure 2B9, B10). Where eggs are visible in the vasculature, cell division radiates outward from the egg
242 and a zone of redifferentiated tissue is apparent around these sites (Figure 2B9, B11, B12). Additionally,
243 the embryo is located in an immature gall chamber (Figure 2B12). Finally, we compared the structure of
244 the gall at 90 dpi to published results to confirm that the artificial infestation approach results in the
245 structure described by Isaias *et al.* (2018). At this stage, the larva has established a mature gall comprising
246 three distinct layers including nutritive tissue that forms the innermost lining of the chamber, followed by
247 a lignified sheath and oxalate crystal deposits (Figure 2B13). The nutritive tissue is approximately six cell
248 layers thick and cells possess a dense, granular cytoplasm (Figure 2B13).

Expression analysis shows defence response

Having seen rapid changes in the host physiology, we then investigated the transcriptional responses of the host following *L. invasa* infestation. Whole genome expression profiles were obtained from high-quality *Eucalyptus* RNA (Table S1). The same tissue types that were used to examine the physical interaction between *L. invasa* and *Eucalyptus* were used for RNA extraction. Sequencing of the samples yielded a minimum of 4.68×10^7 reads per sample with 81-97% mapped. DESeq2 analysis identified 2140, 1003 and 1193 genes showing significant differential expression between control and infested samples at 1, 2 and 3 dpi, respectively (Supplementary File S2). In each case more genes showed up-regulated expression than down-regulated.

At 1 dpi, up-regulated genes are enriched for defence-related GO terms including phytohormone-mediated signalling pathways, oxidative stress and secondary metabolism (Figure 3A). Responses to abscisic acid (ABA) and JA are prevalent, particularly ABA and JA which are enriched throughout the series (Figure 3A1). The observation that genes related to ABA and JA signalling are apparent over the time points suggests that these hormones may act as important regulators of the plant defence response against this pest. Responses to auxin and ethylene (ET) as well as biosynthesis of ET and JA are apparent at 1 dpi, whilst responses to salicylic acid (SA) are apparent at 3 dpi (Figure 3A1). There is also a sustained response to oxidative stress over all three time points suggesting that the plant-type hypersensitive response may be involved which corresponds to the observed ROS accumulation at oviposition sites (Figure 3A2). Similarly, up-regulation of phenylpropanoid biosynthesis-related genes corresponds to the increasing concentration of phenolic compounds (Figure 3A3). GO terms related to the biosynthesis or response to phenolic derivatives are also observed here. Further analysis of phenylpropanoid biosynthetic

genes revealed up-regulation of the pathway, particularly leading to the synthesis of lignin monomers, consistently from 1 dpi to 3 dpi (Figure 3B).

The GO terms also indicate a down-regulation of genes relating to growth and development such as cell proliferation at 1 dpi (Figure 3A4). Additionally, we observe up-regulation of carbohydrate metabolism and nitrate transport (Figure 3A4). Finally, the enriched GO terms also suggest cellular processes that may promote host susceptibility including up-regulation of toxin catabolism suggesting a decrease in the concentration of insecticidal chemicals in the proximal tissues. The former may also contribute to defence by enabling the breakdown of insect-secreted toxins.

Ten transcription factor subfamilies show enrichment at 1 dpi

We identified 248 differentially expressed TF-encoding genes (Supplementary File S3) across the time points that are putatively involved in regulating the *Eucalyptus* responses to oviposition. We further tested whether specific subfamilies of TFs were up- or down-regulated at coordinated times following oviposition. Here we consider orthologous genes that share a common *A. thaliana* annotation as individual members of a TF subfamily. Ten subfamilies, comprising 40 up-regulated genes, showed enrichment at 1 dpi (adjusted p-value ≤ 0.05), including *EgrATAF1, EgrMYB15, EgrMYB36, EgrMYB102*, *EgrMYC2*, *EgrRAP2.1, EgrRAP2.6L, EgrWRKY28*, *EgrWRKY6* and *EgrWRKY75* (Figure 4).

Co-expression and transcription factor binding site enrichment analyses reveal putative biological pathways regulated by transcription factors

We investigated biological processes that may be regulated by the TFs and putatively contribute to gall development. The 40 DEGs belonging to the ten enriched TF subfamilies were used as baits to generate a co-expression network. The expression matrix encompassed data from this study and from publicly available *Eucalyptus*-biotic stress transcriptome analyses including responses to fungus (*C. austroafricana*), oomycete (*P. cinnamomi*) and *L. invasa*. The network includes genes that were co-expressed with the bait genes and were differentially expressed in this study to reduce noise. The network comprises 656 nodes and 3003 edges (maximum correlation ≥0.8) displayed as Cytoscape's prefuse force directed layout (Figure 5). Two functional modules, comprising 75% of the network nodes, were identified suggesting related functionality between cluster members, which was supported by GO term enrichment. The remainder of the network includes small clusters (≤15 nodes) that do not show enrichment for GO terms or TFBS but may be regulated by their local bait TFs.

Module 1 (Figure 5, teal) is the largest in the network and is enriched for defence-associated GO terms. These include responses to ABA, SA, ET and JA, the oxidative burst, phenylpropanoid biosynthesis and systemic acquired resistance. This module includes up-regulated phenylpropanoid biosynthetic genes (orange nodes) observed in Figure 2B as well as several pathogenesis-related such as *EgrPR1* and *EgrPR4* which are markers of the SA and JA pathways, respectively. Module 1 also comprises 25 of the enriched TF subfamily members, including *EgrATAF1, EgrMYB15, EgrMYB36, EgrMYB120, EgrMYC2, EgrWRKY6, EgrWRKY28, EgrWRKY75, EgrRAP2.1* and *EgrRAP2.6L* suggesting that they may regulate similar biological processes or that a higher resolution of data is needed to distinguish which processes are regulated by the TFs. TFBS enrichment analysis identified enriched motifs (*A. thaliana*) in this module including NAC and WRKY highlighting possible binding sites for the bait genes *ATAF1*, *WRKY6*, *WRKY28* and *WRKY75* (Figure 5) further supporting the putative regulatory role of these TFs in the response.

Module 2 (Figure 5, light green) includes four *EgrMYB102* bait genes and one *EgrMYB36*. Interestingly, three of the baits are exclusively differentially expressed following *L. invasa* oviposition on resistant and susceptible host genotypes based on this study and currently available datasets (Mangwanda *et al.*, 2015; Oates *et al.*, 2015; Meyer *et al.*, 2016). These baits are co-expressed with 73 genes where 83% of them only show differential expression in response to *L. invasa* from this study and/or Oates *et al.* (2015) but not other *Eucalyptus*-biotic stress interactions (Supplementary File S4) and are enriched for responses to nitrate and lipid transport, suggesting a specific role in response to *L. invasa*. This cluster also showed enrichment for MYB TFBSs suggesting a regulatory role for *EgrMYB36* and *EgrMYB102* in this module (Supplementary File S5). The results suggest that this module may play an important role in the *Eucalyptus* response to the gall wasp.

Discussion

This study investigated the *L. invasa* oviposition-induced responses of *Eucalyptus* over time. Physiological responses are apparent within one hour of egg deposition and include scarring, ROS accumulation and plant cell lysis putatively caused by the oviposition fluid. Extensive transcriptional reprogramming is apparent at the earliest time point of 1 dpi. DEGs are enriched for defence- and gall development-related biological processes, many of which are reflected in the histological analysis. Results suggest that the phytohormones JA and ABA as well as ten TF subfamilies may play important regulatory roles in this interaction. Members of these TF subfamilies (40 genes in total) were co-expressed with genes that were divided into two modules and ten gene clusters or individuals putatively involved in defence and gall development. The modules also showed enrichment of TFBSs, including *NAC, WRKY* and *MYB*, which supports the regulatory role of these TFs in the *Eucalyptus-L. invasa* interaction. Finally, we show the co-occurrence of phenolics, ROS and auxin transcriptional responses, which are essential components for gall

344 development, suggesting that the *L. invasa* egg and oviposition fluid are responsible for initiating galling
345 in this system.
346
347 *Leptocybe gall induction*
348
349 ROS accumulation is apparent here within one hour of *L. invasa* oviposition and increases over time
350 (Figure 2A). Gene enrichment and up-regulation of certain key genes in the time series, such as respiratory
351 burst oxidase homologs D and F (*EgrRBOHD, EgrRBOHF*), support the onset of the defence-related
352 oxidative burst (Gouhier-Darimont *et al.*, 2013). Furthermore, *WRKY75* was shown to be involved in ROS
353 accumulation leading to leaf senescence (Guo *et al.*, 2017) and increased resistance to *Xanthomonas*
354 *campestrix* in cabbage (Choi *et al.*, 2016). However, no ovicidal effects manifest and continued embryonic
355 development and gall initiation are observed. Interestingly, *RBOHD* is also commonly up-regulated in
356 plant-galling insect interactions (Takeda *et al.* 2019) suggesting that its function in ROS generation is
357 necessary for galling. ROS participate in numerous biological processes, including cell division and cell wall
358 modification (Considine & Foyer, 2014). Isaias *et al.* (2015) proposed that gall-inducing insects can redirect
359 the defence-related oxidative burst towards cell wall modification to facilitate gall development.
360
361 We demonstrate accumulation of phenolics and up-regulation of the phenylpropanoid biosynthetic
362 pathway genes from 1 dpi at the oviposition site. This pathway is an important source of anti-oxidant
363 molecules, cell wall components and secondary metabolites commonly found in galled tissues (Bedetti *et*
364 *al.*, 2014; Suzuki *et al.*, 2015; Hall *et al.*, 2017). Finally, genes involved in auxin signalling, such as auxin-
365 responsive GH3- and SAUR-like auxin-responsive protein-encoding genes, show differential expression
366 within 1 dpi and are also observed in module 1. These genes are co-expressed with several cell wall
367 modifying genes, such as expansins, that may be involved in differentiation of gall-specific tissues (Formiga

368 *et al.*, 2013; Suzuki *et al.*, 2015). Auxin is generally accepted to be an important regulator in gall
369 development (Tooker & Helms, 2014). Li *et al.* (2017) showed that *L. invasa* pre-larval galls accumulate
370 phenolics, tannins, flavonoids and auxins, further validating our hypothesis that components necessary
371 for gall formation are apparent within 1 dpi.
372
373 Module 2 in the network comprises numerous *L. invasa* oviposition-responsive genes (based on available
374 data) that are enriched for responses to nitrate and lipid transport (Figure 5). A number of these genes,
375 such as *3-ketoacyl-CoA synthase 1* and disease-responsive dirigent-like proteins, are involved in wax
376 biosynthesis, cuticle development and cell wall modifications, respectively (Kosma *et al.* 2010).
377 Microscopy and ultrastructural studies of the wheat-Hessian fly interaction revealed a widespread
378 increase in plant surface porosity (Kosma *et al.* 2010). These modifications may facilitate nutrient
379 accumulation in the surrounding cells that form the nutritive tissue, such as observed in the immature gall
380 (Figure 2).
381
382 Gallers are known to modify the source-sink relationship of their hosts, often resulting in increased
383 availability of sugars, lipids and proteins in the nutritive tissue of the gall chamber (Saltzmann *et al.*, 2008;
384 Nabity *et al.*, 2013; Huang *et al.*, 2014; Ferreira *et al.*, 2015). Here, transcriptional responses suggest that
385 *L. invasa* egg and oviposition can manipulate the host's metabolism as early as 1 dpi. Genes involved in
386 carbohydrate metabolism and nitrate transport are up-regulated at 1 dpi. Module 1 includes numerous
387 genes involved in carbon and nitrogen metabolism. These results are supported by Li *et al.* (2017) *L. invasa*
388 induced significant increases in carbon and nitrogen concentrations in pre-larval galls.
389
390 We observed the redifferentiation of vascular tissue into gall-specific cells at 7 dpi (Figure 2B). The
391 orientation of this dividing zone parallel to the oviposition fluid suggests that the oviposition fluid contains

elicitors that stimulate cell division. Where eggs are present, immature gall chambers are formed around the embryo. Numerous plant-galler interactions describe the larva as the life stage that is involved in gall formation; however, egg- and oviposition fluid-induced cell division in host tissues has been previously reported (Leggo & Shorthouse, 2006; Sliva & Shorthouse, 2006) and causes the formation of a complete gall in at least one instance (Barnewall & de Clerck-Floate, 2012). This is the first case of egg- and oviposition fluid-induced gall formation for Hymenoptera.

Coordination of the defence response

The results suggest that ABA, JA and ET are particularly involved in regulating the *Eucalyptus-L. invasa* interaction. The JA signalling pathway is considered to be the major regulator of plant-insect interactions, including initial oviposition and later larval life stages (Erb & Reymond, 2019). Furthermore, JA also plays an important role in the wounding response, an unavoidable consequence of many oviposition behaviours (Reymond, 2013). Here, one of the enriched TF subfamilies, *MYC2*, is a master regulator of the JA pathway and of the crosstalk between various phytohormone signalling cascades (Kazan & Manners, 2013). Additionally, both *WRKY28* and *WRKY75* have been shown to promote plant resistance through JA/ET-dependent signaling pathways (Wu & Wang, 2011; Chen *et al.*, 2013).

The plant must correctly integrate different signals to elicit an appropriate response (Jones & Dangl, 2006). *EgrWRKY6* may provide one route for consolidating recognition signals in this interaction. Three *EgrWRKY6s* are located in module 1 which is enriched for WRKY binding sites in the promoters of the co-expressed genes suggesting an important regulatory role for this subfamily in response to *L. invasa* oviposition. In *Nicotiana attenuata*, this gene differentiates wounding from *Manduca sexta* feeding following recognition of oral elicitors and potentiates JA levels and defences during extended herbivore

attack (Skibbe *et al.*, 2008). These TFs may function similarly in this interaction by prioritising an insect-specific response.

Two enriched MYB transcription factor subfamilies, *EgrMYB102* and *EgrMYB36*, were identified. *Myzus persicae* (green peach aphid) feeding on *A. thaliana* induced expression of *MYB102* resulting in ET-dependent susceptibility to aphids (Zhu *et al.*, 2018). However, over-expression of *AtMYB102* promoted resistance following *Pieris rapae* (cabbage white butterfly) feeding and functions by integrating dehydration signals caused by caterpillar-induced wounding (Denekamp & Smeekens, 2003; De Vos *et al.*, 2006). *AtMYB102* induced the expression of defence- and cell wall modification-related genes (De Vos *et al.*, 2006). In the second case, *At*MYB36 has been shown to be responsible for directing the expression of genes necessary to correctly position and deposit lignin to build Casparian strips in roots (Kamiya *et al.*, 2015). Interestingly, ectopic expression of *AtMYB36* is sufficient to synthesise Casparian strips in plant tissues that do not normally possess these structures (Kamiya *et al.*, 2015). *AtMYB36* has also been shown to regulate the transition from cell proliferation to differentiation in roots (Liberman *et al.*, 2015). Module 2 of the network includes three *EgrMYB102* orthologs as well as *EgrMYB36* co-expressed with genes related to wax, cuticle and cell wall modifications and 83% of the genes show *L. invasa*-induced differential expression based on currently available data. This suggests that module 2 may be involved in the cell wall adjustment that is crucial for gall development.

The plant cell wall also serves as one of the earliest barriers encountered by pests and pathogens (Erb & Reymond, 2019). Two of the enriched TF subfamilies, *MYB102* and *MYB15*, have been shown to regulate basal immunity by promoting cell wall reinforcement during biotic stresses (Denekamp & Smeekens, 2003; De Vos *et al.*, 2006; Chezem *et al.*, 2017).

ABA is the primary regulator of responses to dehydration which is linked to wounding that causes localised water loss (Reymond, 2013). ABA also functions synergistically with JA in mediating plant defence against insects (Ton *et al.*, 2009). The enriched TF subfamily, *EgrATAF1*, promotes ABA-dependent biotic stress resistance but suppresses ABA-dependent abiotic stress resistance (Ton *et al.*, 2009). *EgrATAF1*-encoding genes are co-expressed with genes enriched for defence related GO terms and closely correlated with *EgrRAP2.1*, which is a drought-inducible, negative regulator of dehydration-responsive elements and ensures fine-tuning of *A. thaliana* abiotic responses. However, Li *et al.* (2017) showed that ABA concentrations are significantly increased in *L. invasa*-infested plants throughout gall development (pre-larval to mature galls) which supports the genes related to ABA responses observed throughout this study. This suggests that ABA participates in *L. invasa* susceptibility, possibly by preventing desiccation of the egg and surrounding tissues.

These results provide a detailed insight into the early transcriptional and morphological responses of *Eucalyptus* to *L. invasa* oviposition. This study significantly improved upon the current model of this interaction by identifying JA, ABA, ET and ten TF subfamilies that putatively regulate the interaction. Functional studies will be required to further evaluate their roles in resistance. We demonstrate that the egg and oviposition fluid initiate gall development possibly by redirecting plant defence-related functions with elicitors. Proteomics and/or metabolomic studies may provide a means for identifying these elicitors and understanding the mechanisms behind plant-galling insect interactions.

Acknowledgements

We acknowledge the following people for their contributions to the study. Plant material and insectarium facilities were provided by Mondi and the Forestry and Agricultural Biotechnology Institute (FABI). We

464 thank Ms Samantha Bush, Mr Joseph Khadile and Mr Celani Nkosi for assistance in collecting infested
465 material and sorting wasps and Dr Krzysztof Polanski for assistance with the bioinformatics analyses.
466
467
468 **References**
469 Atkin O.K., Botman B. & Lambers H. (1996). The relationship between the relative growth rate and
470 nitrogen economy of alpine and lowland Poa species. *Plant, Cell and Environment*, 19(11),
471 1324-1330.
472 Ament K., Kant M.R., Sabelis M.W., Haring M.A. & Schuurink R.C. (2004). Jasmonic Acid Is a Key Regulator
473 of Spider Mite-Induced Volatile Terpenoid and Methyl Salicylate Emission in Tomato. *Plant*
474 *Physiology* 135: 2025–2037.
475 Andrews S.F. (2014). A quality control tool for high throughput sequence data. Babraham Bioinformatics.
476 Balbyshev N.F., Lorenzen J.H. (1997). Hypersensitivity and egg drop: A novel mechanism of host-plant
477 resistance to Colorado potato beetle (Coleoptera: Chrysomelidae). *Journal of Economic*
478 *Entomology* 90: 652–657.
479 Barnewall E.C. & de Clerck-Floate R.A. (2012). A preliminary histological investigation of gall induction in
480 an unconventional galling system. *Arthropod-Plant Interactions* 6: 449–459.
481 Bedetti C.S., Modolo L.V. & Isaias R.M. dos S. (2014). The role of phenolics in the control of auxin in galls
482 of *Piptadenia gonoacantha* (Mart.) MacBr (Fabaceae: Mimosoideae). *Biochemical Systematics*
483 *and Ecology* 55: 53–59.
484 Benjamini Y. & Hochberg Y. (1995). Controlling the False Discovery Rate: A Practical and Powerful
485 Approach to Multiple Testing. *Source Journal of the Royal Statistical Society. Series B*
486 *(Methodological) Journal of the Royal Statistical Society. Series B J. R. Statist. Soc. B* 57: 289–300.
487 Berens M.L., Berry H.M., Mine A., Argueso C.T. & Tsuda K. (2017). Evolution of Hormone Signaling

Networks in Plant Defense. *Annual Review of Phytopathology* 55: 401–425.

Berlyn G., Miksche J. & Sass J. (1976). Botanical microtechnique and cytochemistry. *Iowa State University Press*: 326.

Bolger A.M., Lohse M. & Usadel B. (2014). Trimmomatic: A flexible trimmer for Illumina sequence data. *Bioinformatics* 30: 2114–2120.

Boller T. & Felix G. (2009). A Renaissance of Elicitors: Perception of Microbe-Associated Molecular Patterns and Danger Signals by Pattern-Recognition Receptors. *Annual Review of Plant Biology* 60: 379–406.

Büchel K., McDowell E., Nelson W., Descour A., Gershenzon J., Hilker M., Soderlund C., Gang D.R., Fenning T. & Meiners T. (2012). An elm EST database for identifying leaf beetle egg-induced defense genes. *BMC Genomics* 13: 1–17.

Carocha V., Hefer C., Cassan-Wang H., Fevereiro P., Myburg A.A., Paiva J.A.P. & Grima-Pettenati J. (2015). Genome-wide analysis of the lignin toolbox of *Eucalyptus grandis*. *New Phytologist* 206: 1297–1313.

Chen X., Liu J., Lin G., Wang A., Wang Z. & Lu G. (2013). Overexpression of *AtWRKY28* and *AtWRKY75* in *Arabidopsis* enhances resistance to oxalic acid and *Sclerotinia sclerotiorum*. *Plant Cell Reports* 32: 1589-1599.

Chezem W.R., Memon A., Li F-S., Weng J-K. & Clay N.K. (2017). SG2-Type R2R3-MYB Transcription Factor MYB15 Controls Defense-Induced Lignification and Basal Immunity in *Arabidopsis*. *The Plant Cell* 29: 1907–1926.

Choi C., Park S., Ahn I., Bae S. & Hwang D.J. (2016). Generation of Chinese cabbage resistant to bacterial soft rot by heterologous expression of Arabidopsis WRKY75. *Plant Biotechnology Reports* 5: 301-307.

Considine M.J. & Foyer C.H. (2014). Redox Regulation of Plant Development. *Antioxidants & Redox*

512 *Signaling* 21: 1305–1326.
513 Denekamp M. & Smeekens S.C. (2003). Integration of Wounding and Osmotic Stress Signals Determines
514 the Expression of the *AtMYB102* Transcription Factor Gene. *Plant Physiology* 132: 1415–1423.
515 Deslandes L. & Rivas S. (2012). Catch me if you can: bacterial effectors and plant targets. *Trends in Plant*
516 *Science* 17: 644–655.
517 Dittrich-Schröder G., Wingfield M.J., Hurley B.P. & Slippers B. (2012). Diversity in *Eucalyptus* susceptibility
518 to the gall-forming wasp *Leptocybe invasa*. *Agricultural and Forest Entomology* 14: 419–427.
519 Dittrich-Schröder G., Hoareau T.B., Hurley B.P., Wingfield M.J., Lawson S., Nahrung H. & Slippers B. (2018).
520 Population genetic analyses of complex global insect invasions in managed landscapes: a
521 *Leptocybe invasa* (Hymenoptera) case study. *Biological Invasions* 20: 2395-2420.
522 Doss R.P., Oliver J.E., Proebsting W.M., Potter S.W., Kuy S., Clement S.L., Williamson R.T., Carney J.R. &
523 DeVilbiss E.D. (2000). Bruchins: Insect-derived plant regulators that stimulate neoplasm
524 formation. *Proceedings of the National Academy of Sciences* 97: 6218–6223.
525 Erb M., Meldau S. & Howe G.A. (2012). Role of phytohormones in insect-specific plant reactions. *Trends*
526 *in Plant Science* 17: 250–259.
527 Erb M. & Reymond P. (2019). Molecular interactions between plants and insect herbivores. *Annual Review*
528 *of Plant Biology* 70: 527-557.
529 Ferreira B.G., Carneiro R.G.S. & Isaias R.M.S. (2015). Multivesicular bodies differentiate exclusively in
530 nutritive fast-dividing cells in *Marcetia taxifolia* galls. *Protoplasma* 252: 1275–1283.
531 Formiga A.T., de Oliveira D.C., Ferreira B.G., Magalhães T.A., de Castro A.C., Fernandes G.W., Isaias R.M.
532 dos S. (2013). The role of pectic composition of cell walls in the determination of the new shape-
533 functional design in galls of *Baccharis reticularia* (Asteraceae). *Protoplasma* 250: 899–908.
534 Fürstenberg-Hägg J., Zagrobelny M. & Bak S. (2013). Plant Defense against Insect Herbivores. *International*
535 *Journal of Molecular Sciences* 14: 10242–10297.

536 Geuss D., Stelzer S., Lortzing T. & Steppuhn A. (2017). *Solanum dulcamara*'s response to eggs of an insect
537 herbivore comprises ovicidal hydrogen peroxide production. *Plant, Cell & Environment* 40: 2663–
538 2677.
539 Giron D., Huguet E., Stone G.N. & Body M. (2016). Insect-induced effects on plants and possible effectors
540 used by galling and leaf-mining insects to manipulate their host-plant. 84: 70–89.
541 Gouhier-Darimont C., Schmiesing A., Bonnet C., Lassueur S. & Reymond P. (2013). Signalling of *Arabidopsis*
542 *thaliana* response to *Pieris brassicae* eggs shares similarities with PAMP-triggered immunity.
543 *Journal of Experimental Botany* 64: 665–674.
544 Griese E., Dicke M., Hilker M. & Fatouros N.E. (2017). Plant response to butterfly eggs: inducibility, severity
545 and success of egg-killing leaf necrosis depends on plant genotype and egg clustering. *Scientific*
546 *Reports* 7: 1–12.
547 Guo P., Li Z., Huang P., Li B., Fang S., Chu J. & Guo H. (2017). A tripartite amplification loop involving the
548 transcription factor WRKY75, salicylic acid and reactive oxygen species accelerates leaf
549 senescence. *The Plant Cell* 29: 2854-2870.
550 Hall C.R., Carroll A.R., Kitching R.L. (2017). A meta-analysis of the effects of galling insects on host plant
551 secondary metabolites. *Arthropod-Plant Interactions* 11: 463–473.
552 Hilker M. & Fatouros N.E. (2015). Plant Responses to Insect Egg Deposition. *Annual Review of Entomology*
553 60: 493–515.
554 Hilker M. & Fatouros N.E. (2016). Resisting the onset of herbivore attack: Plants perceive and respond to
555 insect eggs. *Current Opinion in Plant Biology* 32: 9–16.
556 Hilker M., Kobs C., Varama M. & Schrank K. (2002). Insect egg deposition induces *Pinus sylvestris* to attract
557 egg parasitoids. *The Journal of Experimental Biology* 205: 455–461.
558 Hogenhout S.A. & Bos J.I.B. (2011). Effector proteins that modulate plant-insect interactions. *Current*
559 *Opinion in Plant Biology* 14: 422–428.

560 Huang M.Y., Huang W.D., Chou H.M., Lin K.H., Chen C.C., Chen P.J., Chang Y.T. & Yang C.M. (2014). Leaf-
561 derived cecidomyiid galls are sinks in *Machilus thunbergii* (Lauraceae) leaves. *Physiologia*
562 *Plantarum* 152: 475–485.
563 Isaias R.M. dos S, Ferreira B.G., Alvarenga D.R. de, Barbosa L.R., Salminen J.P. & Steinbauer M.J. (2018).
564 Functional compartmentalisation of nutrients and phenolics in the tissues of galls induced by
565 *Leptocybe invasa* (Hymenoptera: Eulophidae) on *Eucalyptus camaldulensis* (Myrtaceae). *Austral*
566 *Entomology* 57: 238–246.
567 Isaias R.M.S., Oliveira D.C., Moreira A.S.F.P., Soares G.L.G. & Carneiro R.G.S. (2015). The imbalance of
568 redox homeostasis in arthropod-induced plant galls: Mechanisms of stress generation and
569 dissipation. *Biochimica et Biophysica Acta* 1850: 1509–1517.
570 Jin J., He K., Tang X., Li Z., Lv L., Zhao Y., Luo J & Gao G. (2015). An *Arabidopsis* transcriptional regulatory
571 map reveals distinct functional and evolutionary features of novel transcription factors. *Molecular*
572 *Biology and Evolution* 32: 1767–1773.
573 Jin J., Tian F., Yang D.C., Meng Y.Q., Kong L., Luo J. & Gao G. (2017). PlantTFDB 4.0: Toward a central hub
574 for transcription factors and regulatory interactions in plants. *Nucleic Acids Research* 45: D1040–
575 D1045.
576 Jin J., Zhang H., Kong L., Gao G. & Luo J. (2014). PlantTFDB 3.0: A portal for the functional and evolutionary
577 study of plant transcription factors. *Nucleic Acids Research* 42: 1182–1187.
578 Jones J.D.G. & Dangl J.L. (2006). The plant immune system. *Nature* 444: 323–329.
579 Kamiya T., Borghi M., Wang P., Danku J.M., Kalmbach L., Hosmani P.S., Naseer S., Fujiwara T., Geldner N.
580 & Salt D.E. (2015). The MYB36 transcription factor orchestrates Casparian strip formation.
581 *Proceedings of the National Academy of Sciences* 112: 10533-10538.
582 Kazan K. & Manners J.M. (2013). MYC2: The master in action. *Molecular Plant* 6: 686–703.
583 Kim D., Pertea G., Trapnell C., Pimentel H., Kelley R. & Salzberg SL. (2013). TopHat2: Accurate alignment

584 of transcriptomes in the presence of insertions, deletions and gene fusions. *Genome Biology* 14:
585 R36.
586 Kosma D.K., Nemacheck J.A., Jenks M.A. & Williams C.E. (2010). Changes in properties of wheat leaf cuticle
587 during interactions with Hessian fly. *The Plant Journal* 63:31-43.
588 Leggo J.J. & Shorthouse J.D. (2006b). Development of stem galls induced by *Diplolepis triforma*
589 (Hymenoptera: Cynipidae) on *Rosa acicularis* (Rosaceae). *Canadian Entomologist* 138: 661–680.
590 Li X.Q., Liu Y.Z., Guo W.F., Solanki M.K., Yang Z.D., Xiang Y., Ma Z.C. & Wen Y.G. (2017). The gall wasp
591 *Leptocybe invasa* (Hymenoptera: Eulophidae) stimulates different chemical and phytohormone
592 responses in two *Eucalyptus* varieties that vary in susceptibility to galling. *Tree Physiology* 37:
593 1208–1217.
594 Liao Y., Smyth G.K. & Shi W. (2014). FeatureCounts: An efficient general purpose program for assigning
595 sequence reads to genomic features. *Bioinformatics* 30: 923–930.
596 Liberman L.M., Sparks E.E., Moreno-Risueno M.A., Petricka J.J., Benfey P.N. (2015). MYB36 regulates the
597 transition from proliferation to differentiation in the *Arabidopsis* root. *Proceedings of the National*
598 *Academy of Sciences* 112: 12099-12104.
599 Little D., Gouhier-Darimont C., Bruessow F. & Reymond P. (2006). Oviposition by Pierid Butterflies Triggers
600 Defense Responses in *Arabidopsis*. *Plant Physiology* 143: 784–800.
601 Love M.I., Huber W. & Anders S. (2014). Moderated estimation of fold change and dispersion for RNA-seq
602 data with DESeq2. *Genome Biology* 15: 1–21.
603 Mangwanda R., Myburg A.A. & Naidoo S. (2015). Transcriptome and hormone profiling reveals *Eucalyptus*
604 *grandis* defence responses against *Chrysoporthe austroafricana*. *BMC Genomics* 16: 1–13.
605 Mendel Z., Protasov A., Fisher N. & La Salle J. (2004). Taxonomy and biology of *Leptocybe invasa* gen. &
606 sp. n. (Hymenoptera: Eulophidae), an invasive gall inducer on *Eucalyptus*. *Australian Journal of*
607 *Entomology* 43: 101–113.

608 Meyer F.E., Shuey L.S., Naidoo S., Mamni T., Berger D.K., Myburg A.A., van den Berg N. & Naidoo S. (2016).
609 Dual RNA-Sequencing of *Eucalyptus nitens* during *Phytophthora cinnamomi* Challenge Reveals
610 Pathogen and Host Factors Influencing Compatibility. *Frontiers in Plant Science* 7: 1–15.
611 Morris J.H., Apeltsin L., Newman A.M., Baumbach J, Wittkop T., Su G., Bader G.D. & Ferrin T.E. (2011).
612 ClusterMaker: A multi-algorithm clustering plugin for Cytoscape. *BMC Bioinformatics* 12: 436.
613 Myburg A.A., Grattapaglia D., Tuskan G.A., Hellsten U., Hayes R.D., Grimwood J., Jenkins J., Lindquist E.,
614 Tice H., Bauer D., *et al.* (2014). The genome of *Eucalyptus grandis*. *Nature* 510: 356–362.
615 Nabity P.D., Haus M.J., Berenbaum M.R. & DeLucia E.H. (2013). Leaf-galling phylloxera on grapes
616 reprograms host metabolism and morphology. *Proceedings of the National Academy of Sciences*
617 110: 16663–16668.
618 Oates C.N., Denby K.J., Myburg A.A., Slippers B. & Naidoo S. (2016). Insect Gallers and Their Plant Hosts:
619 From Omics Data to Systems Biology. *International Journal of Molecular Sciences* 17.
620 Oates C.N., Külheim C., Myburg A.A., Slippers B. & Naidoo S. (2015). The Transcriptome and Terpene
621 Profile of *Eucalyptus grandis* Reveals Mechanisms of Defense Against the Insect Pest, *Leptocybe*
622 *invasa*. *Plant and Cell Physiology* 56: 1418–1428.
623 R Core Team (2018). R: A language and environment for statistical computing. R Foundation for Statistical
624 Computing, Vienna, Austria. URL https://www.R-project.org/.
625 Reymond P. (2013). Perception, signaling and molecular basis of oviposition-mediated plant responses.
626 *Planta* 238: 247–258.
627 Saltzmann K.D., Giovanini M.P., Zheng C., & Williams C.E. (2008). Virulent Hessian Fly Larvae Manipulate
628 the Free Amino Acid Content of Host Wheat Plants. *Journal of Chemical Ecology* 34: 1401–1410.
629 Shannon P., Markiel A., Ozier O., Baliga N.S., Wang J.T., Ramage D., Amin N., Schwikowski B. & Ideker T.
630 (2003). Cytoscape: A software Environment for integrated models of biomolecular interaction
631 networks. *Genome Research* 13: 2498–2504.

632 Skibbe M., Qu N., Galis I. & Baldwin I.T. (2008). Induced Plant Defenses in the Natural Environment:
633 *Nicotiana attenuata* WRKY3 and WRKY6 Coordinate Responses to Herbivory. *the Plant Cell Online*
634 20: 1984–2000.
635 Sliva M.D. & Shorthouse J.D. (2006). Comparison of the development of stem galls induced by *Aulacidea*
636 *hieracii* (Hymenoptera : Cynipidae) on hawkweed and by *Diplolepis spinosa* (Hymenoptera :
637 Cynipidae) on rose. *Canadian Journal of Botany-Revue Canadienne de Botanique* 84: 1052–1074.
638 Stone G.N. & Schönrogge K. (2003). The adaptive significance of insect gall morphology. *Trends in Ecology*
639 *and Evolution* 18: 512–522.
640 Stuart J. (2015). Insect effectors and gene-for-gene interactions with host plants. *Current Opinion in Insect*
641 *Science* 9: 56–61.
642 Suzuki A.Y.M., Bedetti C.S. & Isaias R.M. dos S. (2015). Detection and distribution of cell growth regulators
643 and cellulose microfibrils during the development of Lopesia sp. galls on *Lonchocarpus cultratus*
644 (Fabaceae). *Botany* 93: 435–444.
645 Takeda S., Yoza M., Amano T., Ohshima I., Hirano T., Sato M.H., Sakamoto T. & Kimura S. (2019).
646 Comparative transcriptome analysis of galls from four different host plants suggests the molecular
647 mechanism of gall development. *PloS one*10.
648 Ton J., Flors V. & Mauch-Mani B. (2009). The multifaceted role of ABA in disease resistance. *Trends in Plant*
649 *Science* 14: 310–317.
650 Tooker J.F. & Helms A.M. (2014). Phytohormone Dynamics Associated with Gall Insects, and their Potential
651 Role in the Evolution of the Gall-Inducing Habit. *Journal of Chemical Ecology* 40: 742–753.
652 Tzfadia O., Diels T., De Meyer S., Vandepoele K., Aharoni A. & Van de Peer Y. (2016). CoExpNetViz:
653 Comparative Co-Expression Networks Construction and Visualization Tool. *Frontiers in Plant*
654 *Science* 6: 1–7.
655 Unsicker S.B., Kunert G. & Gershenzon J. (2009). Protective perfumes: the role of vegetative volatiles in

plant defense against herbivores. *Current Opinion in Plant Biology* 12: 479–485.

De Vos M., Denekamp M., Dicke M., Vuylsteke M., Van Loon LC, Smeekens S.C.M. & Pieterse C.M.J. (2006). The *Arabidopsis thaliana* transcription factor AtMYB102 functions in defense against the insect herbivore *Pieris rapae*. *Plant Signaling and Behavior* 1: 305–311.

Wu P. & Wang Z. (2011). Molecular mechanisms regulating Pi-signaling and Pi homeostasis under OsPHR2, a central Pi-signaling regulator, in rice. *Frontiers in Biology* 6: 242-245.

Zhu L., Guo J., Ma Z., Wang J. & Zhou C. (2018). *Arabidopsis* transcription factor MYB102 increases plant susceptibility to aphids by substantial activation of ethylene biosynthesis. *Biomolecules* 8.

Figure Legends

Figure 1. Methodological overview of the *L. invasa* infestation applied to susceptible *Eucalyptus grandis* x *E. camaldulensis* ramets to obtain one biological replicate at a single time point of infested and control samples. (**A**) Three target sites (shoot tip, first and second leaves as well as their respective petioles, indicated in blocks) were selected per ramet. Each target site was exposed to five, newly emerged *L. invasa* females (infested) from 11:00 to 12:00 to minimise diurnal variation. Wasp movement was restricted using plastic bags enclosed around the target sites. Material was excised approximately 5 mm around the oviposition scars (dotted lines). Each biological replicate (BR1) comprised pooled material from three different ramets (Ramet 1, 2 and 3). (**B**) Control samples at 1 and 2 dpi were treated similarly with empty bags enclosed around the target sites. For 1 and 2 dpi control samples, the shoot tip, midrib and lower third of the midrib (dotted line) were pooled across the ramets (all potential targets where females were likely to lay eggs) (**C**) For 3 dpi controls, the shoot tip (top), midrib (middle) and petiole (bottom) were pooled separately.

Figure 2. *Leptocybe invasa* oviposition-induced physiological responses leading to gall development. (**A1**) Oviposition occurs along the midrib and induces a necrotic response and ROS accumulation (arrows, stained with DAB) within one hour. (**A2-A5**) At 1 dpi, scarring is apparent and is visible until 7 dpi. ROS accumulation increases until 3 dpi with a similar intensity at 7 dpi and is co-localised with the scarred tissue. (**B1, B2**) Comparisons of cross and longitudinal sections (dual-stained with Safranin O and Fast Green FCF) of control tissue at 7 dpi versus (**B3-B5**) infested tissue indicate that eggs are deposited singly into the vasculature in an alternating pattern, ie. alternately on the left and right side of the midrib. The oviposition fluid (red-stained fluid) is spread throughout the oviposition site and has a rapid degradative effect on the surrounding tissue. The egg is round and anchored to the tissue with a pedicle that may also

absorb water and nutrients from the surrounding tissue. (**B6-B8**) The egg elongates by 1 dpi and becomes roughly aligned with the vascular tissue. This shape and orientation is also present at 2 and 3 dpi. Phenolic accumulation (purple-stained compounds) occurs by 1 dpi proximal to the oviposition site on the ventral leaf surface and is sustained over the time series. (**B9-B12**) At 7 dpi, extensive cell division is visible parallel to localisation of oviposition fluid at the oviposition sites as well as proximal to the eggs in the vascular tissue and decreases with distance. The developing embryos, still enclosed by the egg membrane, are surrounded by dividing cells within the vasculature indicating tissue redifferentiation. An immature gall has formed with the egg located in the larval chamber. (**B13**) The mature gall comprises three distinct tissue layers surrounding the larva. The nutritive tissue forms the inner-most lining of the larval chamber. It is approximately 5 cell layers thick and cells possess a granular cytoplasm. A lignified sheath surrounds the nutritive tissue. The final layer includes oxalate crystal deposits. VT: vascular tissue, OG: oil gland, E: egg, OF: oviposition fluid, OS: oviposition site, cd: cell degradation, P: pedicel, PH: phenolics, IG: immature gall, div: cell division, L: larva, NT: nutritive tissue, LS: lignified sheath, OC: oxalate crystals. Blocks indicate areas shown at higher magnification.

Figure 3. *Leptocybe invasa* oviposition-induced transcriptomic responses leading to gall development. (**A1-A4**) Heatmaps showing selected GO terms of up- (red) and down-regulated (blue), significantly differentially expressed genes at 1, 2 and 3 dpi (adjusted p-value ≤ 0.05). Colour bar indicates significance. (**B**) The phenylpropanoid pathway indicating heat maps of the gene expression of biosynthesis-related genes at 1, 2 and 3 dpi. Red indicates up-regulation, blue indicates down-regulation. Coloured boxes indicate the position of the genes in the pathway. Pathway adapted from Carocha *et al.* (2015).

Figure 4. Expression profiles of genes belonging to ten transcription factor subfamilies showing enrichment at 1 dpi. Heatmaps indicate the $\log_2$ (fold change) of differentially expressed transcription

714 factors as well as their absolute expression values (VST) under normal conditions in the *E. grandis* tissue
715 atlas (https://eucgenie.org). Colour bar indicates individual members of the transcription factor
716 subfamilies.
717
718 **Figure 5. Co-expression network of genes with clusters and bait genes shown.** Baits are shown as ovals,
719 *L. invasa*-responsive nodes are shown as diamonds and genes are colour-coded according to module
720 membership. Coloured blocks indicate selected overrepresented GO biological process terms and
721 enriched transcription factor binding sites for their respective modules. Orange nodes in module 1
722 represent phenylpropanoid biosynthetic genes. Edges indicate positive correlation between nodes with
723 length indicative of correlation coefficient.
724
725 **Supplementary File S1.** Microscopy images of *Leptocybe invasa* oviposition-induced physiological
726 responses.
727
728 **Supplementary File S2.** Summary of significantly differentially expressed genes and their annotations
729 identified at 1, 2 and 3 dpi, GO enrichments and phenylpropanoid metabolism related genes.
730
731 **Supplementary File S3.** Summary of significantly differentially expressed transcription factor-encoding
732 genes at 1, 2 and 3 dpi.
733
734 **Supplementary File S4.** Summary of co-expression module members, correlations and GO enrichment.
735
736 **Supplementary File S5.** Summary of enriched transcription factor binding motifs in network module 1, 2
737 and 3.

Author Contributions

CNO conceived of the study, performed all experiments, collected sample material, analysed all data, drafted the manuscript and prepared all figures. SN conceived of and supervised the study as well as helped draft the manuscript. KJD, AAM and BS helped draft the manuscript. The authors declare no conflict of interest.

Funding

This work was supported by the Department of Science and Technology grant for Forest Genomics and Biotechnology, the South African National Research Foundation Grant for Y-rated researchers [UID105767 to SN]; Incentive funding for rated researchers [UID95807]; Technology and Human Resources for Industry Programme (THRIP; Grant ID 96413); and the Technology Innovation Agency (TIA) Forest Molecular Genetics Cluster Programme. Opinions expressed and the conclusion arrived at are those of the authors and are not necessarily to be attributed to the NRF.

Disclosures

762

763 The authors have no conflicts of interest to declare.

764

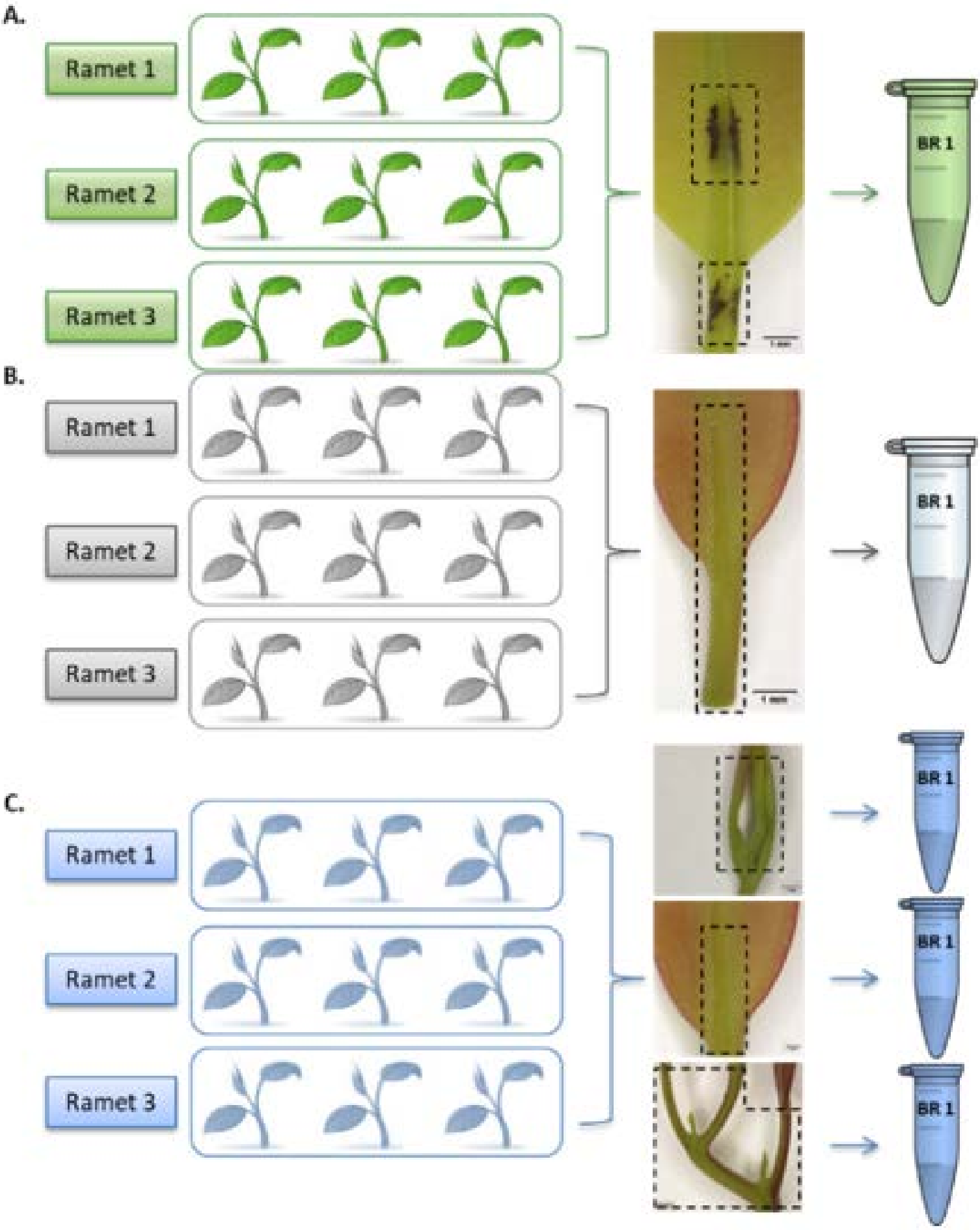
A.
Ramet 1
Ramet 2
Ramet 3
BR 1
B.
Ramet 1
Ramet 2
Ramet 3
BR 1
C.
Ramet 1
Ramet 2
Ramet 3
BR 1
BR 1
BR 1

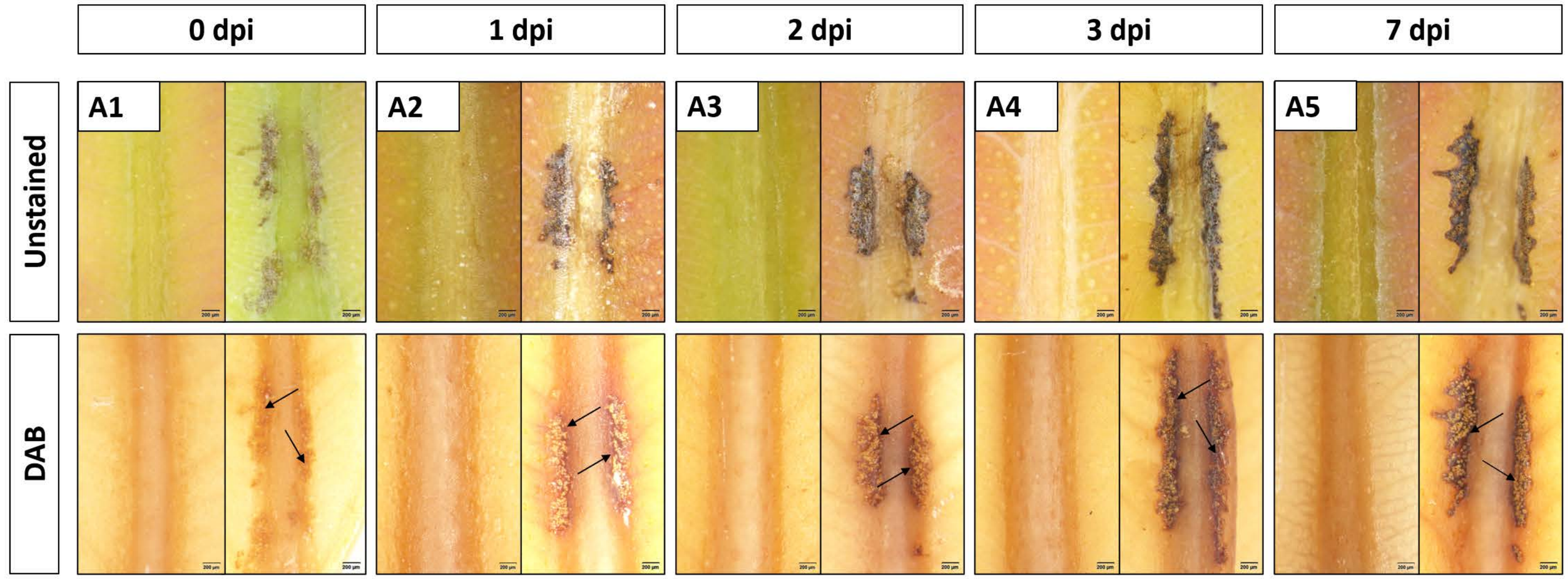
0 dpi
1 dpi
2 dpi
3 dpi
7 dpi
Unstained
DAB
A1
A2
A3
A4
A5
B1.
VT
B2.
VT
OG
B3. 0 dpi
OG
OF
VT
E
OS
OS
cd
B4. 0 dpi
OG
OF
OF
OF
OS
E
cd
cd
B5. 0 dpi
OF
OF
P
E
cd
cd
B6. 1 dpi
E
OG
E
OS
OF
PH
B7. 2 dpi
E
OF
B8. 3 dpi
E
E
OF
OF
PH
B9. 7 dpi
OF
OG
OF
OF
E
IG
div
OG
B10. 7 dpi
OG
div
div
div
div
OS
OF
B11. 7 dpi
PH
B12. 7 dpi
E
IG
B13. 90 dpi
OC
NT
L
LS
PH

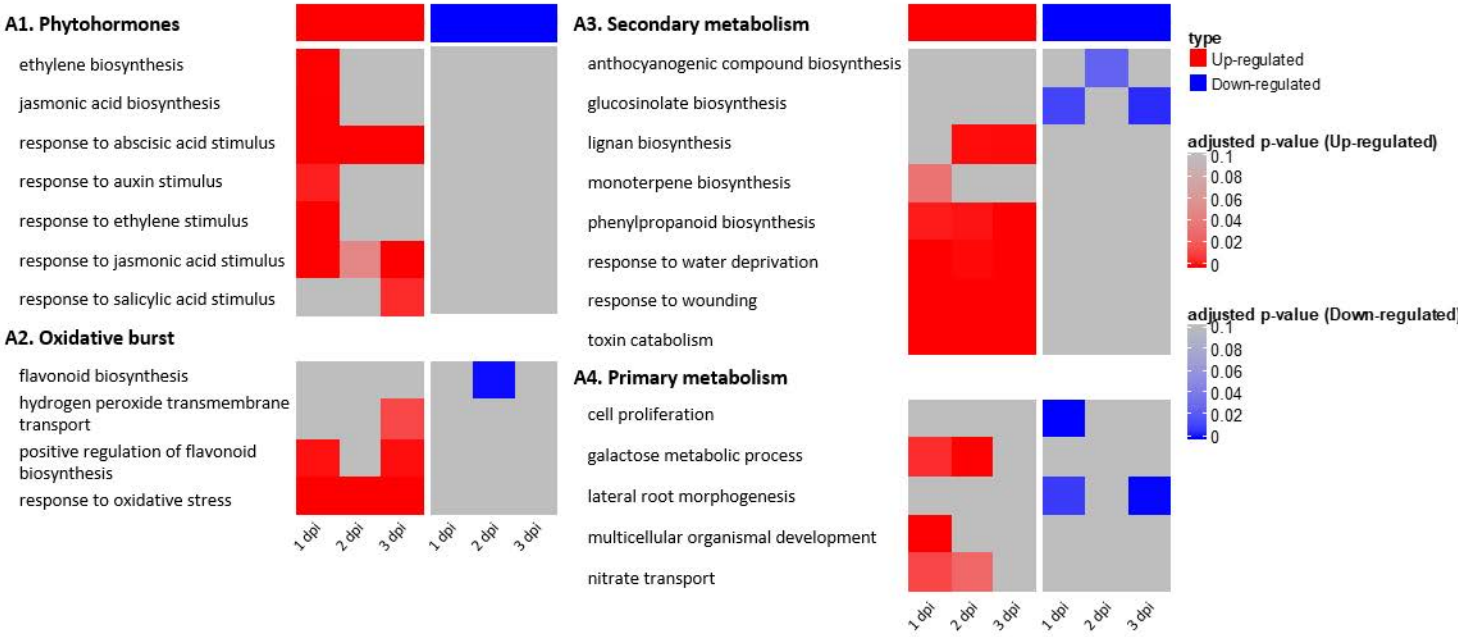
A1. Phytohormones
ethylene biosynthesis
jasmonic acid biosynthesis
response to abscisic acid stimulus
response to auxin stimulus
response to ethylene stimulus
response to jasmonic acid stimulus
response to salicylic acid stimulus
A2. Oxidative burst
flavonoid biosynthesis
hydrogen peroxide transmembrane transport
positive regulation of flavonoid biosynthesis
response to oxidative stress
1 dpi
2 dpi
3 dpi
A3. Secondary metabolism
anthocyanogenic compound biosynthesis
glucosinolate biosynthesis
lignan biosynthesis
monoterpene biosynthesis
phenylpropanoid biosynthesis
response to water deprivation
response to wounding
toxin catabolism
A4. Primary metabolism
cell proliferation
galactose metabolic process
lateral root morphogenesis
multicellular organismal development
nitrate transport
type
Up-regulated
Down-regulated
adjusted p-value (Up-regulated)
0.1
0.08
0.06
0.04
0.02
0
adjusted p-value (Down-regulated)
0.1
0.08
0.06
0.04
0.02
0

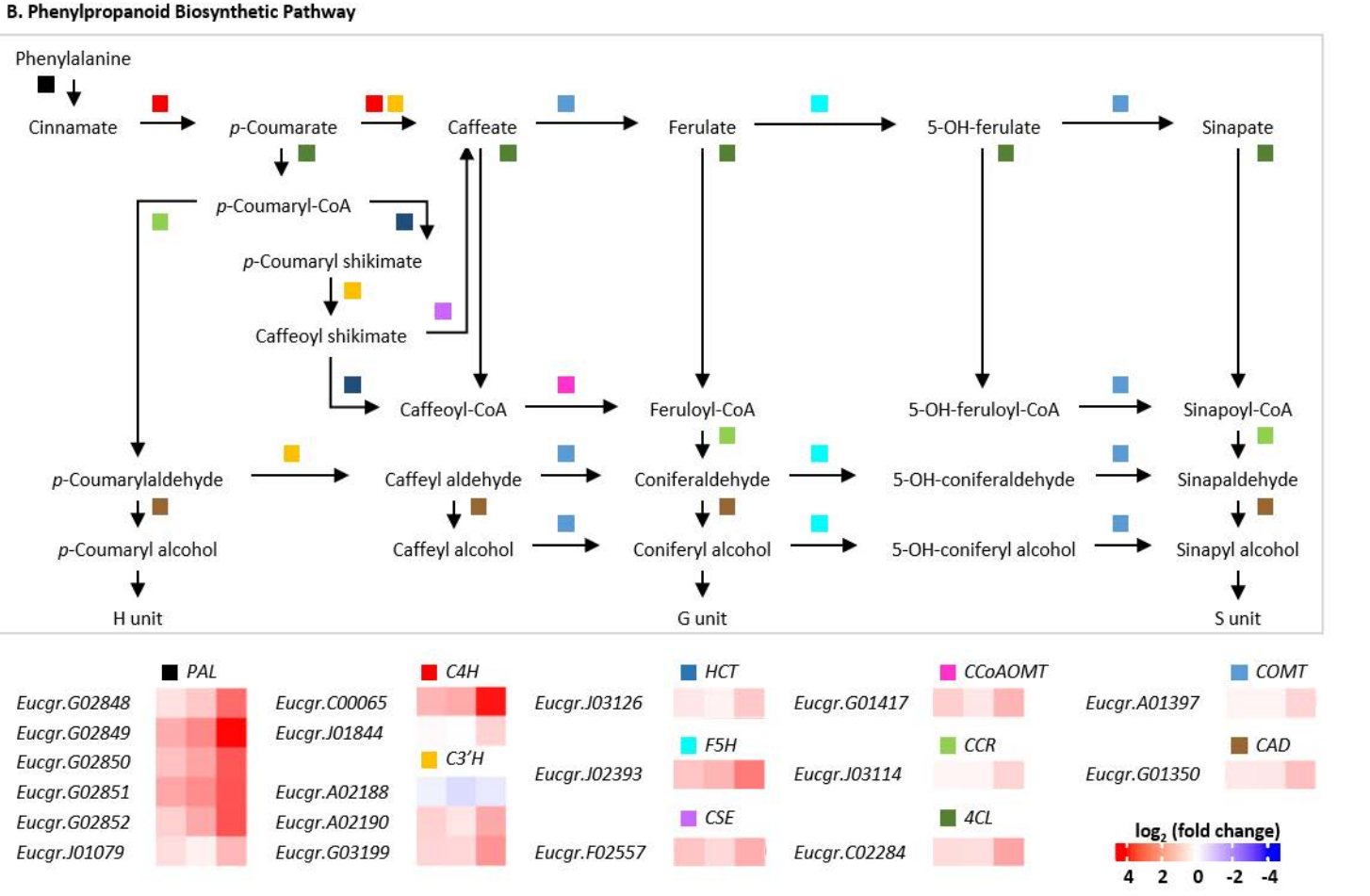
B. Phenylpropanoid Biosynthetic Pathway
Phenylalanine
Cinnamate
p-Coumarate
Caffeate
Ferulate
5-OH-ferulate
Sinapate
p-Coumaryl-CoA
p-Coumaryl shikimate
Caffeoyl shikimate
Caffeoyl-CoA
Feruloyl-CoA
5-OH-feruloyl-CoA
Sinapoyl-CoA
p-Coumarylaldehyde
Caffeyl aldehyde
Coniferaldehyde
5-OH-coniferaldehyde
Sinapaldehyde
p-Coumaryl alcohol
Caffeyl alcohol
Coniferyl alcohol
5-OH-coniferyl alcohol
Sinapyl alcohol
H unit
G unit
S unit
PAL
Eucgr.G02848
Eucgr.G02849
Eucgr.G02850
Eucgr.G02851
Eucgr.G02852
Eucgr.J01079
C4H
Eucgr.C00065
Eucgr.J01844
C3'H
Eucgr.A02188
Eucgr.A02190
Eucgr.G03199
HCT
Eucgr.J03126
F5H
Eucgr.J02393
CSE
Eucgr.F02557
CCoAOMT
Eucgr.G01417
CCR
Eucgr.J03114
4CL
Eucgr.C02284
COMT
Eucgr.A01397
CAD
Eucgr.G01350
log2 (fold change)
4
2
0
-2
-4

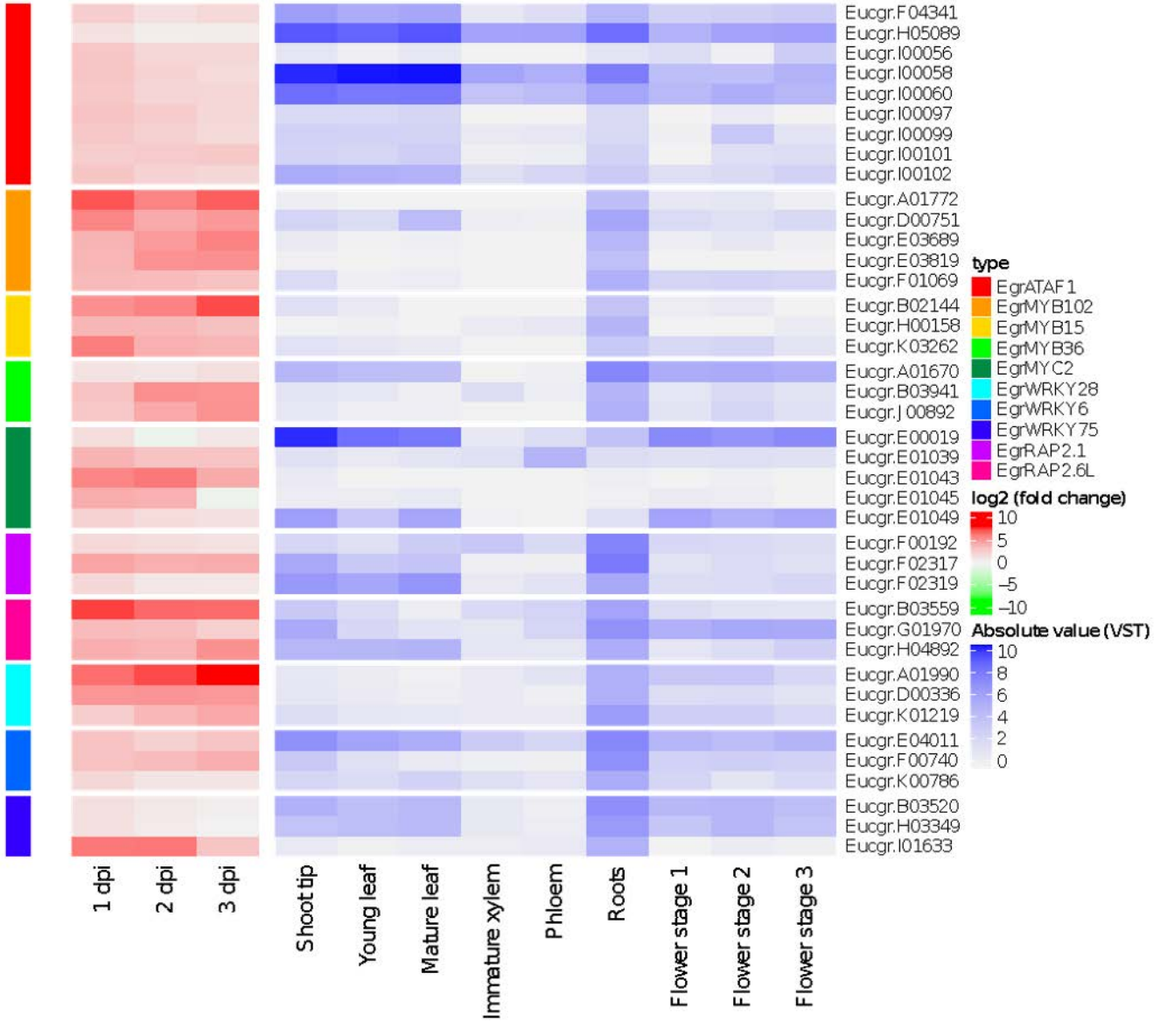
Eucgr.F04341
Eucgr.H05089
Eucgr.I00056
Eucgr.I00058
Eucgr.I00060
Eucgr.I00097
Eucgr.I00099
Eucgr.I00101
Eucgr.I00102
Eucgr.A01772
Eucgr.D00751
Eucgr.E03689
Eucgr.E03819
Eucgr.F01069
Eucgr.B02144
Eucgr.H00158
Eucgr.K03262
Eucgr.A01670
Eucgr.B03941
Eucgr.J00892
Eucgr.E00019
Eucgr.E01039
Eucgr.E01043
Eucgr.E01045
Eucgr.E01049
Eucgr.F00192
Eucgr.F02317
Eucgr.F02319
Eucgr.B03559
Eucgr.G01970
Eucgr.H04892
Eucgr.A01990
Eucgr.D00336
Eucgr.K01219
Eucgr.E04011
Eucgr.F00740
Eucgr.K00786
Eucgr.B03520
Eucgr.H03349
Eucgr.I01633
1 dpi
2 dpi
3 dpi
Shoot tip
Young leaf
Mature leaf
Immature xylem
Phloem
Roots
Flower stage 1
Flower stage 2
Flower stage 3
type
EgrATAF1
EgrMYB102
EgrMYB15
EgrMYB36
EgrMYC2
EgrWRKY28
EgrWRKY6
EgrWRKY75
EgrRAP2.1
EgrRAP2.6L
log2 (fold change)
10
5
0
−5
−10
Absolute value (VST)
10
8
6
4
2
0

Module 1	
GO terms	**Adj p-val**
❖ phenylpropanoid biosynthetic process	<0.001
❖ regulation of response to nutrient levels	0.007
❖ response to abscisic acid stimulus	<0.001
❖ response to ethylene stimulus	<0.001
❖ response to jasmonic acid stimulus	<0.001
❖ response to oxidative stress	0.001
❖ response to salicylic acid stimulus	0.04
❖ systemic acquired resistance	<0.001
Transcription factor binding sites	**E value**
○ *WRKY*	<0.001
	<0.001
	<0.001
○ *NAC*	<0.001
	<0.001
	<0.001

Module 2	
GO terms	**Adj p-val**
❖ lipid transport	0.003
❖ nitrate transport	0.03
❖ response to nitrate	0.02
Transcription factor binding sites	**E value**
○ *MYB*	<0.001
	<0.001
	<0.001